Evolution of Fiber Morphologies during Poly (acrylonitrile) Electrospinning

Jian Fang, Hongxia Wang, Haitao Niu, Tong Lin, Xungai Wang*

Summary: In this study, we used a facile approach to examine the evolution of fiber morphologies during electrospinning, via solidifying the newly electrospun polyacrylonitrile (PAN) nanofibers in an ethanol bath at different electrospinning distances (2 cm to 10 cm). It has been observed that a massive jet-thinning took place at the initial stage of whipping instability, followed by uneven fiber-stretching. The fiber-stretching at the later whipping stage was mainly concentrated on beaded fiber sections, which improved the uniformity of the resultant fibers.

Keywords: electrospinning; evolution; morphology; polyacrylonitrile; whipping instability

Introduction

Electrospinning is a very useful technique to produce polymeric nanofibers for diverse applications,[1–7] this technique involves stretching a polymer fluid under a strong electric field into dry or semidry filaments, which are deposited randomly on a grounded collector forming a non-woven nanofiber mat. Improved electrospinning processes have been able to control the fiber alignment,[8–11] to produce bicomponent nanofibers,[12–15] or to form porous[16,17] and other novel fiber structures.[18–20]

The fiber stretching during electrospinning is a fast and incessant process which can be divided into three consecutive stages[1,3]: jet initiation, whipping instability and fiber deposition. From the initial jet to dry fibers, the fiber stretching process takes place in milliseconds.[21] Although extensive works have been undertaken to understand the effects of operating parameters (e.g. applied voltage, spinning distance, flow rate of polymer solution) and initial material properties (e.g. solution viscosity, conductivity, surface tension, solvent volatility) on the electrospinning process and resultant fiber morphology,[22–26] little is known on how the jet/filament changes its morphology in the whipping period. As a result of lacking in-depth understanding of the fiber stretching behavior, the control of electrospinning process and fiber morphology has been based on adjusting operating parameters and initial solution properties.

To observe the fiber stretching process, a high-speed video camera has been used, and a single-jet stretching mechanism accompanied with helical jet/filament movement has been evident[21,27–29]. However, the relatively low image resolution of the optical microscope makes it difficult to accurately record and quantify the filament morphology change during electrospinning. Collecting the as-spun nanofibers at different spinning distances could be another option, but it is only suitable for relatively long electrospinning distance, because collecting fibers at a short distance normally results in polymer film.[30,31]

In this study, we used a facile approach to solidify electrospun polyacrylonitrile (PAN) fibers at different spinning distances, by depositing the newly electrospun PAN fibers in an ethanol solution. The evolution of fiber morphologies during electrospinning was thus established. Also, the bead formation mechanism was

Centre for Material and Fibre Innovation, Deakin University, Geelong, VIC 3217, Australia
E-mail: tongl@deakin.edu.au

elucidated via comparing the morphology changes in electrospinning uniform and non-uniform (beaded) fibers.

Experimental Part

Polyacrylonitrile (M_w 86,200 g/mol), *N, N*-dimethylformamide (DMF) and ethanol were obtained from Aldrich and used as received. The fiber morphology was observed under a scanning electron microscope (SEM, LEO 1530 microscope), and the average fiber diameter was calculated based on the SEM images with the aid of image analysis software (Image*Pro* plus4.5). The electric field strength was calculated with 2-D limited elementary method using software Femlab*3.1*.

A purpose-built electrospinning apparatus used in this work is shown in Figure 1. The polymer solution was put into a 5 ml plastic syringe and connected to a high voltage power supply (ES30P, Gamma High Voltage Research) via a metal syringe needle (21 Gauge). A round copper disk (diameter = 8 cm) used as the grounded electrode was placed in a plastic flask (inner diameter = 9 cm and depth = 15 cm) right underneath the syringe needle (nozzle). The distance between the tip of nozzle and the copper disk was fixed at 15 cm. Before electrospinning, ethanol was added into the plastic flask so that the as-spun fibers were directly electrospun into ethanol bath before reaching the grounded electrode, and the distance between the nozzle tip and ethanol surface (d) was changed via adjusting the volume of ethanol.

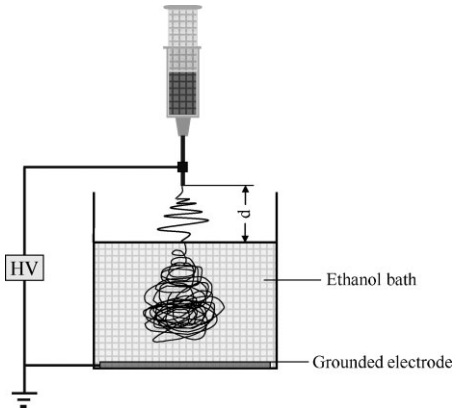

Figure 1.
Apparatus for electrospinning.

During electrospinning, the flow rate of the PAN solution was controlled at 1.0 ml/hr using a digital syringe pump (KD scientific). The applied voltage was kept at 18.0 kV, and the distance between the needle tip and ethanol surface was set in the range of 2∼10 cm.

The nanofiber samples for SEM observation were prepared by transferring small amount of collected nanofibers onto SEM sample holder using conductive double side stick tape. And all the samples were sputter coated with a thin layer of gold (5∼10 nm) to reduce electron charging effects before observation.

Results and Discussion

Electrospinning a polymer solution can result in different fiber morphologies, such as individual beads, beads-on-string structure and bead-free fibers, depending on the polymer concentration used. As shown in Figure 2, electrospinning 5 wt% PAN/DMF solution using a normal electrospinning apparatus[23] resulted in beads-on-string fibers, while the fibers turned bead-free and uniform when the PAN concentration was increased to 7 wt%.

When an ethanol bath was placed between the nozzle and the collector, the as-stretched jet/filament went into the ethanol before reaching the grounded electrode. Once the jet/filament was immersed in the ethanol, it was solidified rapidly due to the insoluble characteristic of PAN in ethanol and a fast solvent exchange between the filament and ethanol.

The filament maintained its original morphology if the PAN concentration is high enough. As we have found that when a PAN/DMF droplet (size about 2 mm) was dropped into an ethanol solution, if the PAN concentration was larger than 4 wt%, a round solid bead was resulted with the

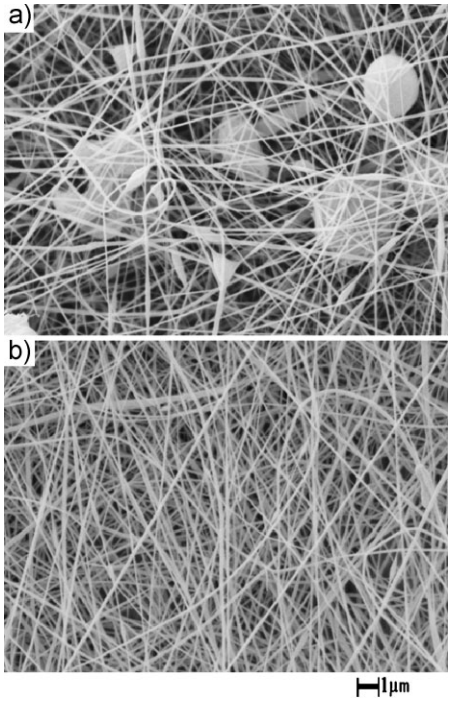

Figure 2.
SEM images of PAN nanofibers electrospun from (a) 5 wt%, and (b) 7 wt% PAN/DMF solution. (Applied voltage = 18 kV and spinning distance = 15 cm).

morphology almost the same as the liquid droplet except for the smaller size, and no polymer split from the droplet. Using ethanol as the coagulator, the as-collected filaments would reflect the morphology of the filaments being stretched with the distance from the nozzle to the surface ethanol bath.

Upon changing the distance between the nozzle tip and the ethanol surface (collecting distance, d) for electrospinning, the fiber morphology at different spinning distance can be observed. For electrospinning 7 wt% PAN solution, the fibers collected at 2 cm showed a beads-on-string structure (Figure 3a). With the increase in the collecting distance, the beaded fibers were always produced until the collecting distance exceeded 7 cm (Figure 3a∼f). Longer collecting distance led to bead-free fibers (Figure 3g∼3i).

The average fiber diameter calculated based on the string sections varied with the collecting distance. As shown in Figure 4, the fibers collected at the spinning distance of 2 cm have an average diameter of 220 ± 30 nm. When the spinning distance was increased from 2 cm to 4 cm, the fiber diameter maintained at the same level, but the diameter distribution became narrow. When the collecting distance was further increased, the fiber diameter reduced slightly. Increasing the collecting distance from 2 cm to 10 cm only led to 30 nm reduction in the average fiber diameter.

Using a long distance microscope, the dimensions of ''Taylor cone'' and the subsequent stable-jet were measured. The length of ''Taylor cone'' was 2∼3 mm, and the length and diameter of the stable-jet were around 6∼10 mm and 200 μm, respectively. After the stable-jet, from 1.3∼2.0 cm, the jet was thinned from around 200 μm to 220 nm. This result suggested that the jet/filament diameter was considerably reduced at the initial stage of whipping instability.

Also, the fiber beads changed their dimension with the collecting distance. As shown in Figure 4, large beads with the average width and length of 960 ± 0.27 nm and 2.72 ± 0.39 μm, respectively, were collected at the distance 2 cm away from the nozzle tip. With the collecting distance increasing from 2 cm to 7 cm, the beads became narrow gradually to 650 nm, however, the length increased initially, but decreased after 3 cm. When the collecting distance was longer than 7 cm, no beads were found among the fibers collected, indicating that the beads were elongated into uniform fibers at the later stage of whipping.

When the 5 wt% PAN/DMF solution was electrospun, beads-on-string fibers were produced even when the collecting distance was as long as 10 cm (Figure 5). The average fiber diameter reduced gradually from 150 ± 25 nm to 105 ± 25 nm when the collecting distance increased from 2 cm to 10 cm (Figure 6). Also, with the increase in the collecting distance, the bead width had a very small change, except that a larger width distribution occurred at the

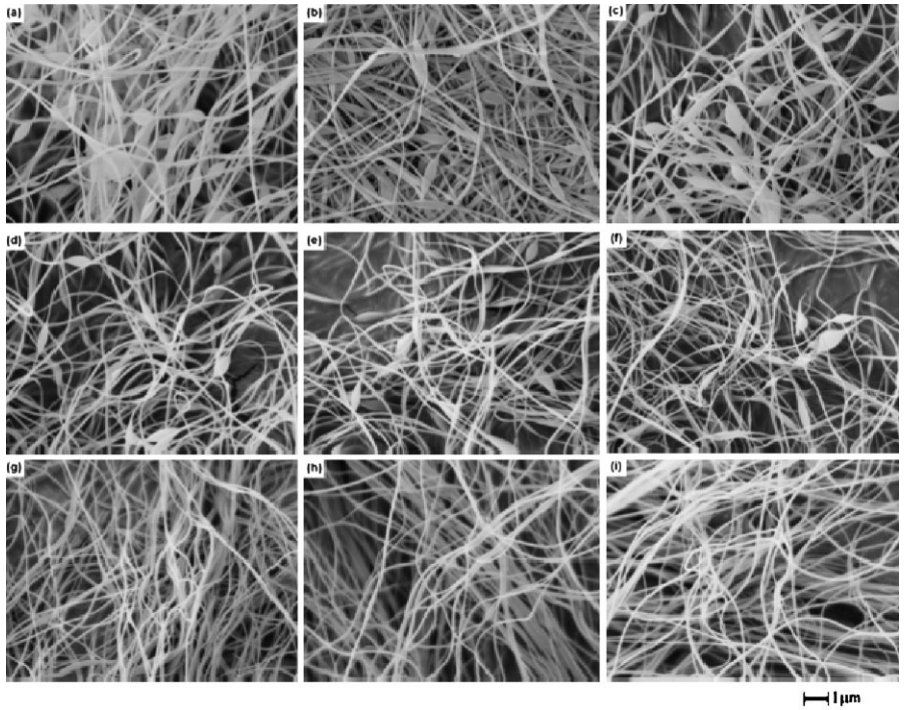

Figure 3.
SEM images of electrospun PAN nanofibers at different collecting distances; (a) 2 cm, (b) 3 cm, (c) 4 cm, (d) 5 cm, (e) 6 cm, (f) 7 cm, (g) 8 cm, (h) 9 cm and (i) 10 cm. (PAN concentration = 7 wt%, applied voltage = 18 kV).

longer electrospinning distance. In contrast, the bead length increased slightly when the collecting distance was increased from 2 cm to 5 cm. The bead became shortened when the collecting distance changed from 6 cm to 7 cm, but maintained its length at the longer collecting distance.

By compassion with the fibers electrospun from 7 wt% PAN solution, the fibers electrospun from 5 wt% PAN solution have a thinner string diameter and bead size. When the collecting distance was larger than 7 cm, beaded fibers were still produced from the 5 wt% PAN solution.

During electrospinning, strong electrostatic interactions between the charged jet/filament and the applied electric field and electrostatic repulsion within the jet

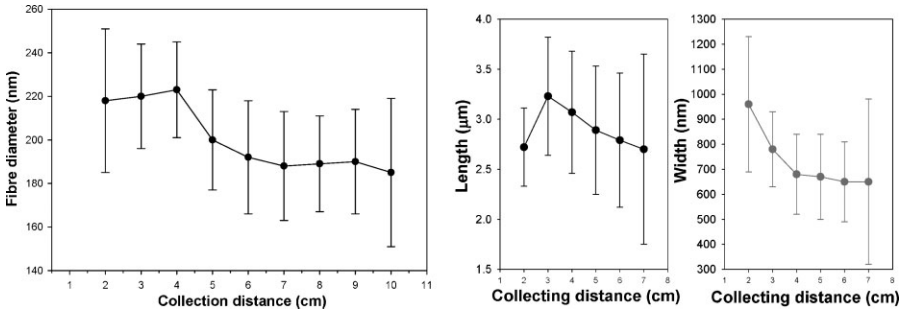

Figure 4.
Average fiber diameter and bead dimension of PAN fibers at different collecting distances. (PAN concentration = 7 wt%).

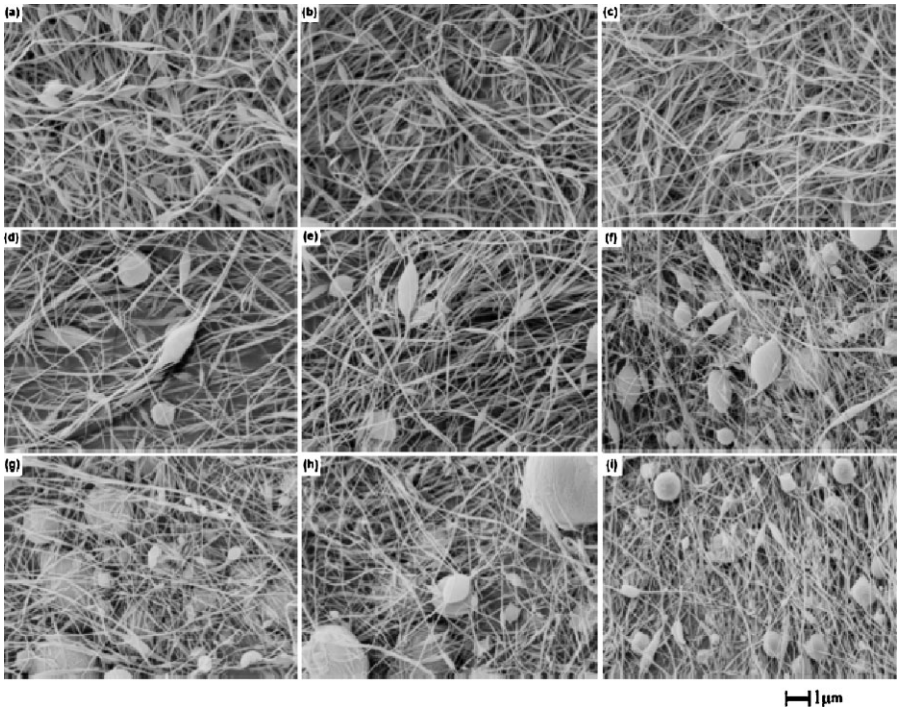

Figure 5.
SEM images of electrospun PAN nanofibers at different collecting distances; (a) 2 cm, (b) 3 cm, (c) 4 cm, (d) 5 cm, (e) 6 cm, (f) 7 cm, (g) 8 cm, (h) 9 cm and (i) 10 cm. (PAN concentration = 5 wt%, applied voltage = 18 kV).

account for the jet instability.[23,32,33] To understand the fiber morphology change, electric field intensity along the direction from the nozzle to the grounded electrode was calculated. As shown in Figure 7, the intensity of electric field decayed rapidly within the first 1.5 cm away from the nozzle, and the rate of decay slowed down considerably afterwards. However, once an ethanol bath was placed between the nozzle and the grounded electrode, the electric field intensity in the ethanol bath reduced to zero rapidly. Also, the height of ethanol bath affected the electric field strength. A higher ethanol bath, corresponding to shorter spinning distance d, led to higher electric field strength. As a result, filament stretched under a higher electric force is thinner than that electrospun without ethanol involved in the electrospinning process. These results also suggest that the current technique may also provide a simple tool to examine the effect of electric field intensity on the changes in fiber morphology in electrospinning.

Since the initial solution properties (conductivity, viscosity and surface tension) have considerable influences on the fiber stretching process, the properties of the two PAN solutions were compared. The surface tension differed little between the solutions. The solution conductivity for 5 wt% and 7 wt% PAN solutions was 33.5 μS/cm and 40.3 μS/cm, respectively. A higher conductivity indicated that the net charge density was higher, hence leading to stronger electrostatic interaction during electrospinning.

A large difference was found in viscosity of the two solutions. The viscosities for 5 wt% and 7 wt% PAN solutions were 58.5 cp and 158.9 cp, respectively. The difference in the viscosity suggested that the two solutions had different mobility. At a higher initial viscosity, the solution was lower in mobility. Although the solutions

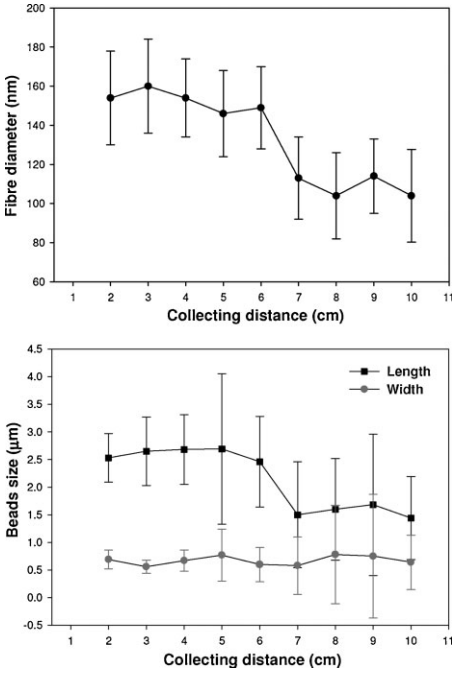

Figure 6.
Average fiber diameter and bead dimension of PAN fibers at different collecting distances. (PAN concentration = 5 wt%).

were all stretched unevenly into beaded filament at the initial whipping stage, the fact that bead-free fibers were electrospun from the polymer solution having lower mobility suggested that the formation of eventual beads-on-string structure was associated with the later stage of whipping movement.

Solvent evaporation during electrospinning also assisted the formation of uniform fibers. As the filament was stretched finer, the highly oriented polymer macromolecules reinforced the filament.[34] Meanwhile, the high surface-to-volume ratio of the fine filament accelerated further evaporating of the solvent. The solvent evaporation also reduced the solution mobility. In comparison, the bead sections had higher mobility than the strings. Because of the lower surface-to-volume ratio, the solvent evaporation from the beaded sections was slower. As a result, the mobility in the beaded sections remained higher than that in the string sections. The formation of beads was dependent on whether the beaded sections were totally stretched into uniform filament at the later stage of whipping.

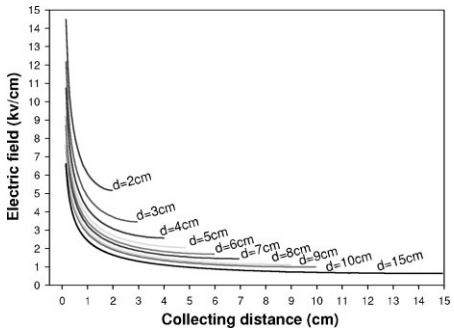

Figure 7.
Calculated electric field strength along the electrospinning area. Nozzle tip (distance = 0), grounded electrode (distance = 15 cm). The *d* is the distance between the tip of nozzle and the ethanol liquid surface. (Applied voltage = 18 kV).

Conclusions

In this study, we have demonstrated that electrospinning a polymer solution into a coagulation solvent before the electrospun fibers reach the grounded electrode is a facile method to understand the fiber morphology change. By collecting the newly electrospun PAN fibers at different electrospinning distances, the evolution of fiber morphologies during electrospinning has been established. It has been found that a massive jet thinning takes place at the initial stage of whipping instability and uneven fiber stretching always happens no matter whether the resultant fibers are uniform or not. The fiber stretching at the later stage of whipping is mainly concatenated on the beaded sections. The formation of beaded fibers is related to low solution mobility.

[1] T. Subbiah, G. S. Bhat, R. W. Tock, S. Parameswaran, S. S. Ramkumar, *Journal of Applied Polymer Science* **2005**, *96*, 557.

[2] W. E. Teo, S. Ramakrishna, *Nanotechnology* **2006**, *17*, R89.
[3] Y. Dzenis, *Science* **2004**, *304*, 1917.
[4] M. R. Abidian, D.-H. Kim, D. C. Martin, *Advanced Materials* **2006**, *18*, 405.
[5] S. R. Bhattarai, N. Bhattarai, H. K. Yi, P. H. Hwang, D. I. Cha, H. Y. Kim, *Biomaterials* **2004**, *25*, 2595.
[6] X. Wang, C. Drew, S.-H. Lee, K. J. Senecal, J. Kumar, L. A. Samuelson, *Journal of Macromolecular Science* **2002**, *A39*, 1251.
[7] J. T. McCann, M. Marquez, Y. Xia, *Journal of the American Chemical Society* **2006**, *128*, 1436.
[8] D. Li, G. Ouyang, J. T. McCann, Y. Xia, *Nano Letters* **2005**, *5*, 913.
[9] S. Zhong, W. E. Teo, X. Zhu, R. W. Beuerman, S. Ramakrishna, L. Y. L. Yung, *Journal of Biomedical Materials Research, Part A* **2006**, *79A*, 456.
[10] P. Katta, M. Alessandro, R. D. Ramsier, G. G. Chase, *Nano Letters* **2004**, *4*, 2215.
[11] W. E. Teo, S. Ramakrishna, *Nanotechnology* **2005**, *16*, 1878.
[12] J. T. McCann, D. Li, Y. Xia, *Journal of Materials Chemistry* **2005**, *15*, 735.
[13] M. Wei, B. Kang, C. Sung, J. Mead, *Macromolecular Materials and Engineering* **2006**, *291*, 1307.
[14] T. McCann Jesse, M. Marquez, Y. Xia, *Nano Letters* **2006**, *6*, 2868.
[15] T. Lin, H. Wang, X. Wang, *Advanced Materials* **2005**, *17*, 2699.
[16] O. O. Dosunmu, G. G. Chase, W. Kataphinan, D. H. Reneker, *Nanotechnology* **2006**, *17*, 1123.
[17] A. C. Patel, S. Li, J.-M. Yuan, Y. Wei, *Nano Letters* **2006**, *6*, 1042.
[18] E. Smit, U. Buttner, R. D. Sanderson, *Polymer* **2005**, *46*, 2419.
[19] H. Pan, L. Li, L. Hu, X. Cui, *Polymer* **2006**, *47*, 4901.
[20] J. Stitzel, J. Liu, J. Lee Sang, M. Komura, J. Berry, S. Soker, G. Lim, M. Van Dyke, R. Czerw, J. Yoo James, A. Atala, *Biomaterials* **2006**, *27*, 1088.
[21] D. H. Reneker, A. L. Yarin, H. Fong, S. Koombhongse, *Journal of Applied Physics* **2000**, *87*, 4531.
[22] T. Lin, J. Fang, H. Wang, T. Cheng, X. Wang, *Nanotechnology* **2006**, *17*, 3718.
[23] T. Lin, H. Wang, H. Wang, X. Wang, *Nanotechnology* **2004**, *15*, 1375.
[24] C. Mit-uppatham, M. Nithitanakul, P. Supaphol, *Macromolecular Chemistry and Physics* **2004**, *205*, 2327.
[25] S. A. Theron, E. Zussman, A. L. Yarin, *Polymer* **2004**, *45*, 2017.
[26] J. M. Deitzel, J. Kleinmeyer, D. Harris, N. C. Beck Tan, *Polymer* **2001**, *42*, 261.
[27] Y. M. Shin, M. M. Hohman, M. P. Brenner, G. C. Rutledge, *Polymer* **2001**, *42*, 9955.
[28] M. M. Hohman, M. Shin, G. Rutledge, M. P. Brenner, *Physics of Fluids* **2001**, *13*, 2221.
[29] A. L. Yarin, S. Koombhongse, D. H. Reneker, *Journal of Applied Physics* **2001**, *89*, 3018.
[30] C. J. Buchko, L. C. Chen, Y. Shen, D. C. Martin, *Polymer* **1999**, *40*, 7397.
[31] J. Kameoka, R. Orth, Y. Yang, D. Czaplewski, R. Mathers, G. W. Coates, H. G. Craighead, *Nanotechnology* **2003**, *14*, 1124.
[32] A. L. Yarin, S. Koombhongse, D. H. Reneker, *Journal of Applied Physics* **2001**, *89*, 3018.
[33] M. M. Hohman, M. Shin, G. Rutledge, M. P. Brenner, *Physics of Fluids* **2001**, *13*, 2201.
[34] A. L. Yarin, *Free Liquid Jets and Films: Hdreodynamics and Rheology*, Wiley, New York **1993**.

